ChemPubSoc Europe

DOI: 10.1002/ejic.201900580

EurJIC European Journal of Inorganic Chemistry

Full Paper

Connector Species

SPECIAL ISSUE

The Potential of the Diphosphorus Complex $[Cp_2W_2(CO)_4(\eta^2\text{-}P_2)]$ as an Organometallic Connecter in Supramolecular Chemistry

Mehdi Elsayed Moussa,[a] Pavel A. Shelyganov,[a] Brian Wegley,[a] Michael Seidl,[a] and Manfred Scheer*[a]

Dedicated to Professor Klaus H. Theopold on the occasion of his 65th birthday.

Abstract: For the first time, the tetrahedral diphosphorus complex $[Cp_2W_2(CO)_4(\mu,\eta^2:\eta^2\text{-}P_2)]$ (Cp = C_5H_5) (**3**) is used as a connecter in supramolecular chemistry. The treatment of **3** with Cu^I halides leads to the formation of the new one-dimensional (1D) linear polymers $[Cu(\mu\text{-}X)\{Cp_2W_2(CO)_4(\mu,\eta^2:\eta^2:\eta^1:\eta^1\text{-}P_2)\}]_n$ {X = Cl (**4**), Br (**5**), I (**6**)}. The coordination polymers (CPs) **4**–**6** are almost insoluble in organic solvents, thus, their ^{31}P MAS-NMR spectra were recorded and found to be remarkably influenced by their solid-state structures. Additionally, we demonstrate that by reacting the Cp-substituted diphosphorus complex $[Cp'_2W_2(CO)_4(\mu,\eta^2:\eta^2\text{-}P_2)]$ {Cp′ = $C_5H_4\{C(CH_3)_3\}$} (**7**) with CuBr, the unprecedented soluble 1D CP $[Cu(\mu\text{-}Br)\{Cp'_2W_2(CO)_4(\mu,\eta^2:\eta^2:\eta^1:\eta^1\text{-}P_2)\}]_n$ (**8**) is obtained. Furthermore, the reactions of **3** with the Ag^I salts $Ag[CF_3SO_3]$ and $Ag[PF_6]$ result in the formation of the oligomeric dicationic species $[Ag_2\{Cp_2W_2(CO)_4(\mu,\eta^2:\eta^2:\eta^2\text{-}P_2)\}_2\{Cp_2W_2(CO)_4(\mu,\eta^2:\eta^2:\eta^1:\eta^1\text{-}P_2)\}_2][X']_2$ {X′ = $[CF_3SO_3]^-$ (**9**), $[PF_6]^-$ (**10**)}.

Introduction

The construction of supramolecular aggregates and networks via the coordination-driven self-assembly of discrete units is an area of growing interest in chemical research.[1] Next to common approaches in this field making use of N-, O- or S-donor-containing organic molecules to link a variety of metal centers,[2] a number of supramolecular assemblies utilizing organometallic building blocks are also reported.[3] Our group contributed to this field in particular by using polyphosphorus (P_n) or polyarsenic (As_n)-donating organometallic ligand complexes with flexible coordination modes as connecters between metal ions.[4] Using these "unusual" linkers, we succeeded in synthesizing 1D, 2D or even 3D coordination polymers (CPs),[5] inorganic fullerene-like supramolecular spherical aggregates[5e,6] and organometallic nanosized capsules.[7] The simplest examples of such P_n complexes are the diphosphorus tetrahedrane complexes $[Cp_2M_2(CO)_4(\mu,\eta^2:\eta^2\text{-}P_2)]$ {M = Mo (**1**), Cr (**2**), Cp = C_5H_5}.[8] These compounds show a similar coordination behavior towards Cu^I halides allowing the formation of 1D CPs with the general formula $[Cu(\mu\text{-}X)\text{-}\{Cp_2M_2(CO)_4(\mu,\eta^2:\eta^2:\eta^1:\eta^1\text{-}P_2)\}]_n$ (X = Cl, Br, I, M = Mo, Cr).[9] However, their reaction with Ag^I salts gave in each case a different product. For example, compound **1** reacts with Ag[TEF] ([TEF] = $[Al\{OC(CF_3)_3\}_4]$)[10] to give the Ag^I dimer $[Ag_2(\eta^2\text{-}\mathbf{1})_2(\mu,\eta^1:\eta^1\text{-}\mathbf{1})_2][TEF]_2$[11] or the 1D polymer $[Ag_2(\mu,\eta^1:\eta^1\text{-}\mathbf{1})_3]_n[TEF]_{2n}$,[5a] depending on the reaction conditions. The treatment of **2** with Ag[TEF] allowed for the formation of the dimer $[Ag_2(\eta^2\text{-}\mathbf{2})(\eta^1\text{-}\mathbf{2})(\mu,\eta^1:\eta^1\text{-}\mathbf{2})_2][TEF]_2$.[12] Yet, due to the very limited stability of the chromium complex **2**,[13] only its molybdenum analogue **1** was frequently used as a building block in supramolecular chemistry. Particularly, its reaction with Ag^I or Cu^I salts and pyridyl-based linkers allowed the isolation of a large variety of unprecedented organometallic-organic hybrid CPs.[14] These results raised the question about the potential of the tungsten analogue $[Cp_2W_2(CO)_4(\mu,\eta^2:\eta^2\text{-}P_2)]$ (**3**) as a connecter in supramolecular chemistry. This compound had been synthesized in 1988 by the Scherer group,[15] but since then, its reactivity has only very limitedly been studied[16] and no supramolecular aggregates featuring this compound as a linking unit have been reported yet. We report herein the low temperature X-ray structures of the P_2 ligand complex **3** and its Cp′-substituted analogue $[Cp'_2W_2(CO)_4(\mu,\eta^2:\eta^2\text{-}P_2)]$ (**7**) (Cp′ = $C_5H_4\{C(CH_3)_3\}$) and show that these compounds can be utilized as connecters in supramolecular chemistry.

Compound **3** reacts with Cu^I halides to give the new 1D polymers $[Cu(\mu\text{-}X)(\mu,\eta^1:\eta^1\text{-}\mathbf{3})]_n$ [X = Cl (**4**), Br (**5**), I (**6**)] and with Ag^I salts to afford $[Ag_2(\eta^2\text{-}\mathbf{3})_2(\mu,\eta^1:\eta^1\text{-}\mathbf{3})_2][X']_2$ {X′ = $[CF_3SO_3]^-$ (**9**), $[PF_6]^-$ (**10**)}. Compound **7** reacts with CuBr affording the unique soluble 1D polymer $[Cu(\mu\text{-}Br)(\mu,\eta^1:\eta^1\text{-}\mathbf{7})]_n$ (**8**). The compounds **4**–**6** and **8**–**10** are the first examples of supramolecular aggre-

[a] *Institut für Anorganische Chemie der Universität Regensburg, 93040 Regensburg, Germany*
E-mail: manfred.scheer@chemie.uni-regensburg.de
https://www.uni-regensburg.de/chemistry-pharmacy/inorganic-chemistry-scheer/index.html
ORCID(s) from the author(s) for this article is/are available on the WWW under https://doi.org/10.1002/ejic.201900580.

gates displaying W_2P_2 organometallic complexes as linking units. Finally, the solid state ^{31}P magic angle spinning (MAS) NMR spectra of the CPs **4**–**6** are recorded and interpreted in correlation to their X-ray structures.

Results and Discussion

The X-ray structure of the P_2 ligand complex $[Cp_2W_2(CO)_4(\mu,\eta^2{:}\eta^2\text{-}P_2)]$ (**3**) was initially measured at room temperature as reported by Mays and co-workers.[17] In order to reliably compare its structural parameters to those of the formed supramolecular aggregates, we measured a single crystal of **3** at 123 K (Table 1, Figure 3). The room temperature reaction of **3** with CuX (X = Cl, Br, I) in a 1:1 mixture of CH_3CN and CH_2Cl_2 leads to the formation of the 1D polymers **4**–**6** as orange crystalline solids in high yields (66–83 %, Scheme 1). Interestingly, the polymers **4**–**6** are the only isolated products regardless of whether a 1:1 or a 2:1 stoichiometric ratio of the reactants **3**:CuX is used in the reactions. The polymers **4**–**6** are insoluble in common organic solvents such as CH_2Cl_2, THF, toluene and *n*-hexane and only sparingly soluble in polar solvents such as CH_3CN. In contrast to their lighter molybdenum- and chromium-based analogues, **4**–**6** are air- and light-stable for at least few days. Single crystals of the compounds **4**–**6**, grown by layering a solution of the appropriate Cu^I halide in CH_3CN over a solution of **3** in CH_2Cl_2, were examined by X-ray crystallography (Figure 1; for further details see the ESI). Compounds **4** and **5** crystallize in the monoclinic space group $P2_1/n$, while **6** crystallizes in the triclinic space group $P\bar{1}$ and contains one molecule of CH_3CN per formula unit. The structures of all the compounds **4**–**6** reveal 1D polymeric frameworks consisting of alternating arrangements of planar four-membered Cu_2X_2 rings and six-membered Cu_2P_4 rings in a slightly chair-like conformation [folding angles; (**4**) 7.59(15), (**5**) 5.09(12), (**6**) 5.82(9)°]. Within the Cu_2P_4 rings, the Cu^I centers possess each a distorted tetrahedral coordination sphere and are bridged by P_2 ligands each adopting a commonly observed $\eta^1{:}\eta^1$-coordination mode. Similar to what was noticed in the free ligand complex **3**, the Cp and CO ligands in the polymers **4**–**6** are located in opposite directions. Selected structural details for the compounds **4**–**6** are listed in Table 1. The P–P bond lengths in **4** [2.093(3) Å] and **5** [2.089(2) Å] are slightly shortened, whereas those of **6** [2.099(2) Å] are

Table 1. Comparison of selected bond lengths [Å] and angles [°] for **4**–**6**.

	3	**4**	**5**	**6**
P–P	2.095(2)	2.093(3)	2.089(2)	2.099(2)
Cu–P		2.276(2)	2.288(1)	2.307(1)
		2.285(2)	2.296(1)	2.303(1)
Cu–X		2.334(2)	2.466(1)	2.604(1)
		2.362(2)	2.477(1)	2.669(1)
P–Cu–P		102.30(8)	102.70(6)	106.25(5)
P–P–Cu		131.60(2)	132.58(6)	133.91(7)
Cu–X–Cu		80.13(6)	76.49(3)	74.18(3)
Cu···Cu···Cu		174.65(5)	176.60(5)	168.35(4)

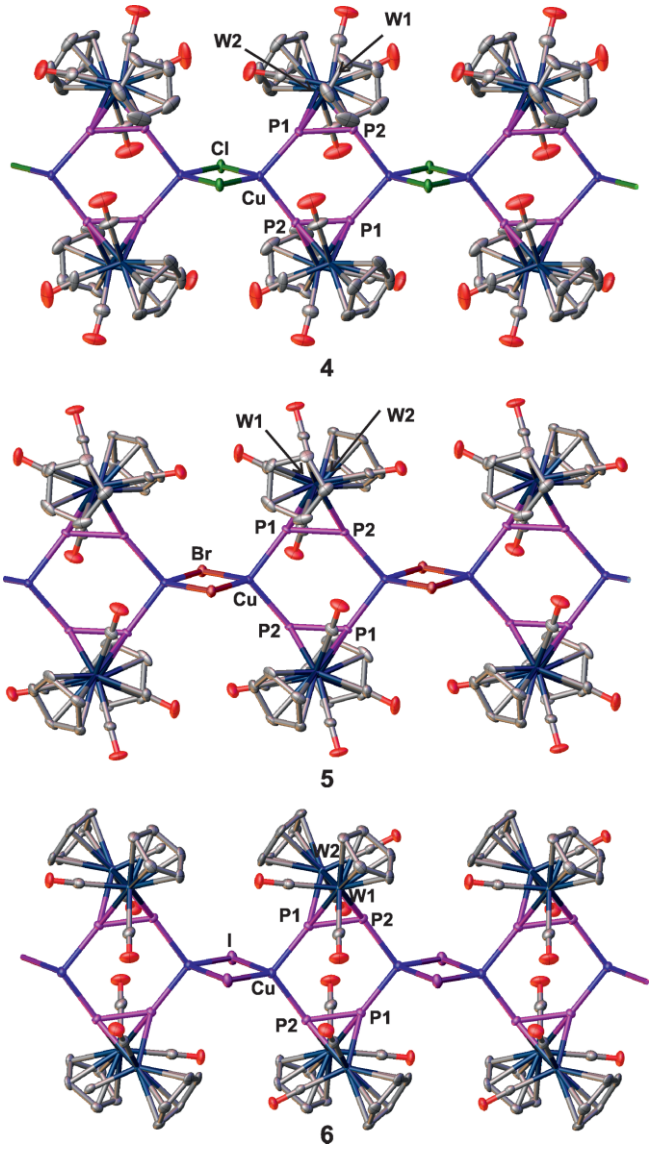

Figure 1. Sections of the 1D CPs **4**–**6** (H atoms have been omitted for clarity).

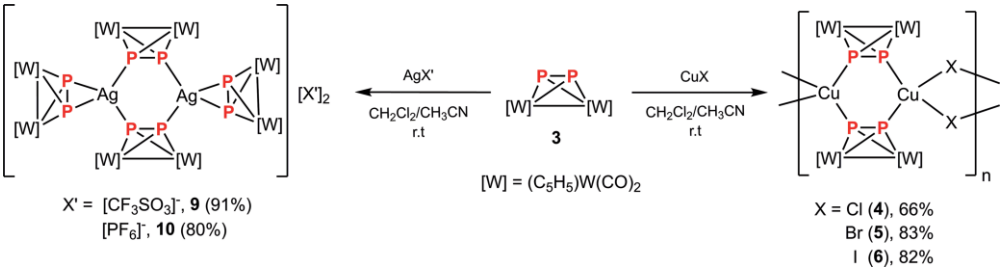

Scheme 1. Reactions of **3** with Cu^I halides, $Ag[CF_3SO_3]$ and $Ag[PF_6]$ leading to the 1D polymers **4**–**6** and the dimers **9** and **10**.

slightly elongated compared to that in the uncoordinated ligand **3** [2.095(2) Å]. The Cu–P bond lengths in the polymers **4**–**6** [2.276(2)–2.307(1) Å] are shorter than those found in similar 1D polymers based on the lighter chromium [2.289(1)–2.333(2) Å] and molybdenum [2.282(2)–2.312(1) Å] analogues **1** and **2**. However, the Cu–X bond lengths in **4**–**6** [2.334(2)–2.669(1) Å] are within the ranges found in the chromium- [2.344(1)–2.675(1) Å] and molybdenum-based [2.348(2)–2.668(1) Å] polymers.[9] As the size of the halogen atom increases, the angles P–Cu–P [102.30(8)° (**4**), 102.70(6)° (**5**), 106.25(8)° (**6**)] and P–P–Cu [131.60(1)° (**4**), 132.58(6)° (**5**), 133.91(7)° (**5**)] increase. The Cu···Cu···Cu angle for the iodide containing polymer **6** [168.35(4)°] is noticeably deviated from linearity as compared to the chloride- or bromide-containing polymers **4** [174.65(5)°] and **5** [176.60(5)°].

Solid-state ^{31}P MAS NMR measurements were performed for the polymers **4**–**6** at room temperature (Figure 2b-d). While the spectrum of the Cu^{I} polymer **6** displays a broad signal centered at about –210 ppm, each of the spectra of the CuCl and CuBr polymers **4** and **5** displays two multiplets near –195 and –320 ppm, which are about 120 ppm apart. The multiplets arise from the combined effect of homonuclear $^{1}J(^{31}P,^{31}P)$ and heteronuclear $^{1}J(^{63/65}Cu,^{31}P)$ indirect spin-spin interactions. The large chemical shift difference between P1 and P2 in **4** and **5**, but not in **6**, can be best interpreted when viewing the structures of the respective Cu_2P_4 rings in each polymer (Figure 2a). As discussed for similar 1D polymers based on **1** and **2**,[9b,9c] this chemical shift difference in **4** and **5** is caused by subtle differences in the orientations of the P1 and P2 atoms with respect to the CO ligands, whose large magnetic anisotropy results in the tremendous difference in the shielding (> 100 ppm). This magnetic inequivalence is also evident from the C_{CO}···P interatomic distances listed in Table 2, showing more carbonyl ligands in close proximity to the P2 atoms than to the P1 atoms, thus resulting in a downfield shift of the ^{31}P MAS NMR signals of P2. On the other hand, the P1 and P2 atoms in **6** have almost similar relative orientations with respect to the CO ligands and show chemical shifts in a similar range to those of the P2 atoms in **4** and **5**.

Table 2. C_{CO}···P interaction distances of the compounds **4**, **5** and **6** [Å].

	4	5	6
C1···P1	2.701	3.130	2.749
C2···P1	3.822	4.017	2.954
C8···P1	3.144	2.688	3.941
C9···P1	4.000	3.836	3.182
C1···P2	3.885	2.780	3.908
C2···P2	3.507	2.885	3.133
C8···P2	2.764	3.881	2.852
C9···P2	2.869	3.502	2.889

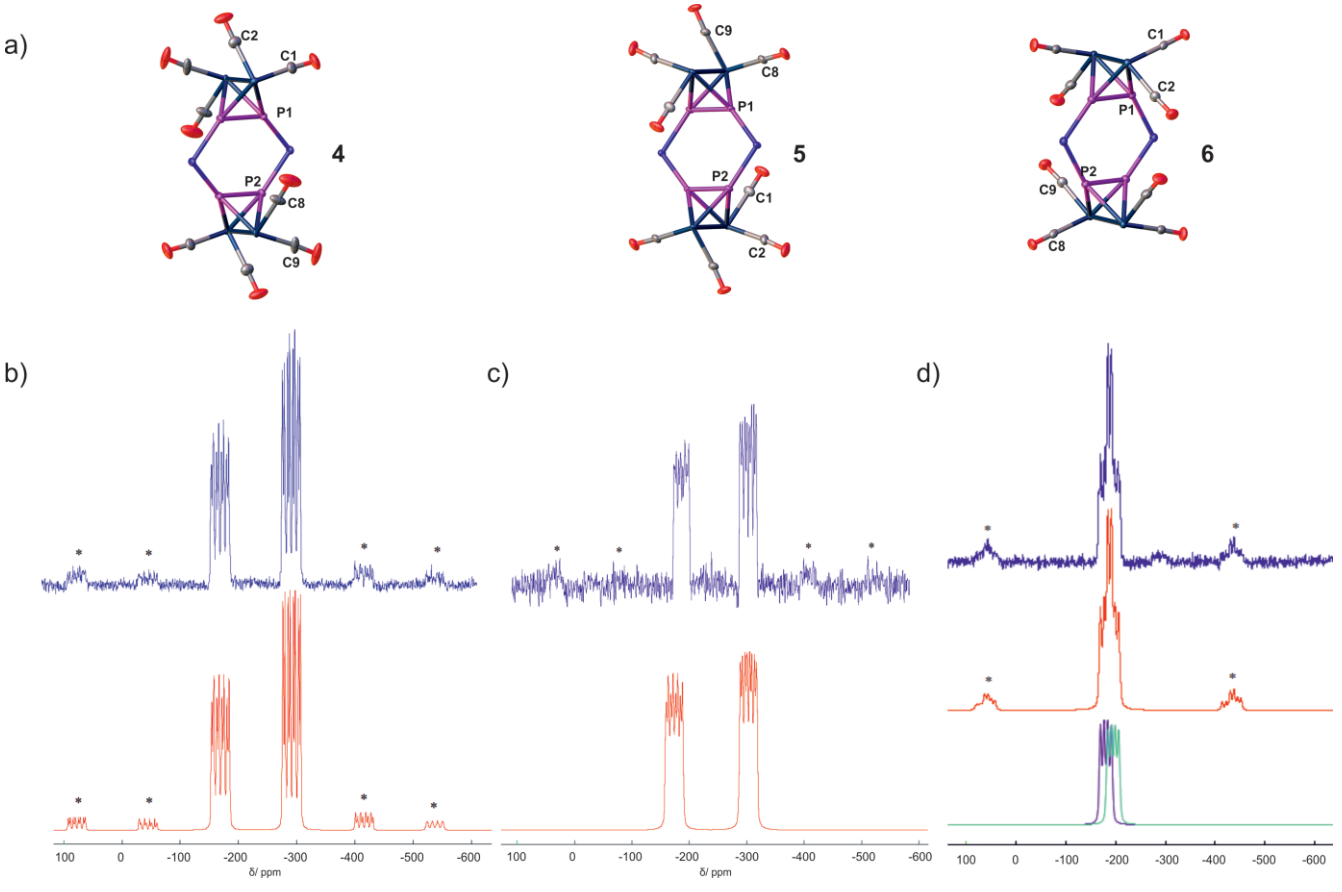

Figure 2. a) View of the Cu_2P_4 rings of the polymers **4**–**6**. (Cp ligands as well as H atoms are omitted for clarity). b,c) Experimental (top) and simulated (bottom) ^{31}P MAS-NMR (121.49 MHz, spinning speed 30 K Hz, room temp.) spectra of **4** and **5**. d) Experimental (top) and simulated (middle) ^{31}P MAS-NMR (121.49 MHz, spinning speed 30 K Hz, r.t.) spectra of **6**, separated contribution of simulated peak (bottom). * = Spinning side bands.

The positive ion ESI-MS spectra of **4**–**6** show a variety of peaks including those assigned to fragments containing Cu^{I} halides and the ligand **3**. However, for all these fragments, the loss of one or more CO ligands is observed, indicating a low stability of **4**–**6** in solution.

Due to the very low solubility of the 1D polymers **4**–**6**, any further characterization in solution was not possible. Thus, the question arose as to whether it is possible to synthesize structurally similar but soluble polymers. Seemingly, the most relevant way in this case is to use a better soluble P_2 complex analogue of **3**. Hence, we investigated the reactivity of the ligand complex $[Cp'_2W_2(CO)_4(\mu,\eta^2{:}\eta^2\text{-}P_2)]$ {Cp′ = $C_5H_4\{C(CH_3)_3\}$} (**7**) as a potential candidate. This compound, which is similar to **3**, was first synthesized by the Scherer group,[15] but it was not to date structurally characterized. Single crystals of **7** were obtained at room temperature from the slow evaporation of a concentrated 1:1 toluene/pentane solution mixture. This compound crystallizes in the monoclinic space group $C2/_c$. Its solid-state structure shows two tungsten atoms in close contact, each bounded by two carbonyl atoms, the *tert*-butylcyclopentadienyl group and two phosphorus atoms in a tetrahedral W_2P_2 framework (Figure 3b).

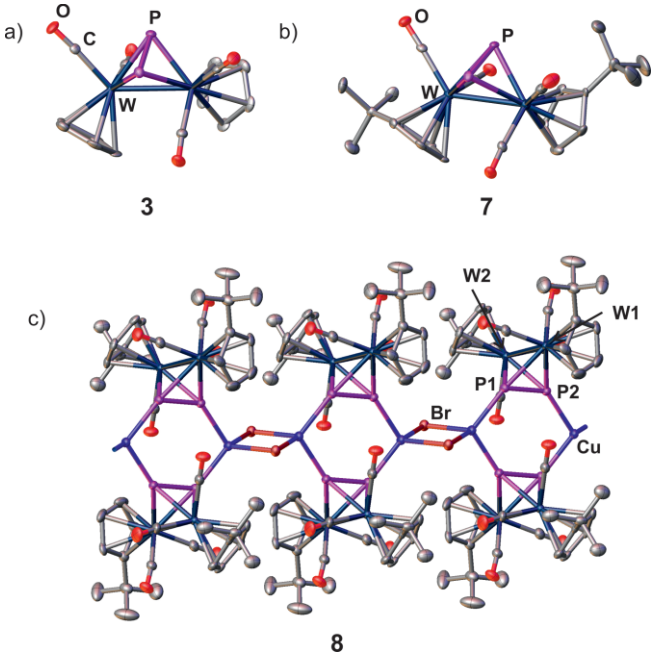

Figure 3. Molecular structures of a) **3** and b) **7** in the crystal. c) Section of the 1D CP **8** (H atoms have been omitted for clarity).

The treatment of **7** with CuBr afforded the 1D CP **8** in excellent yield (86 %, Scheme 2). Single crystals of **8** were grown by layering a solution of the crude reaction mixture with *n*-pentane at 4 °C. Compound **8** crystallizes in the monoclinic space group $C2/_c$. The X-ray structure analysis of **8** reveals a 1D polymeric framework similar to that of **5** in such a way that it consists of six-membered Cu_2P_4 rings linked by two bridging μ-Br ions (Figure 3c). Selected structural details for **8** are listed in Table 3. The Cu_2P_4 rings in **8** show a larger deviation towards a chair-like conformation than those in **5** {folding angle; (**8**) [10.70(10), (**5**) 5.09(12)°]}. The P–P bond length in **8** [2.097(2) Å] is similar to that of **7** [2.098(2) Å] and slightly longer than that in the polymer **5** [2.089(2) Å]. The Cu–P bond lengths in **8** [2.294(2)–2.311(2) Å] are also longer than those found in **5** [2.288(1)–2.296(1) Å].

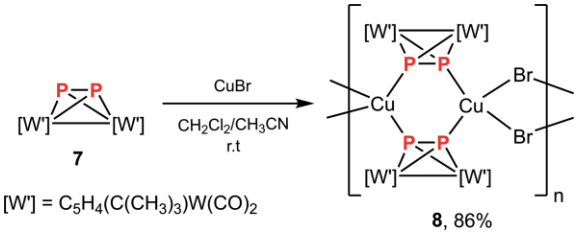

Scheme 2. Reactions of **7** with CuBr leading to the 1D polymer **8**.

Table 3. Comparison of selected bond lengths [Å] and angles [°] for **7**–**10**.

	7	**8** (M= Cu)	**9** (M= Ag)	**10** (M= Ag)
P–P	2.098(2)	2.097(2)	2.103(3)	2.109(2)
			2.166(2)	2.159(2)
M–P		2.294(2)	2.470(2)	2.473(1)
		2.311(2)	2.667(2)	2.683(1)
M–M		2.334(2)	4.630	4.558
		2.362(2)		
P1–M–P2		102.30(8)	48.52(5)	48.15(3)
P3–M–P4			117.45(6)	120.24(4)

As intended, in contrast to the polymers **4**–**6**, the 1D polymer **8** is soluble in common organic solvents such as THF, CH_2Cl_2 and CH_3CN. In fact, **8** is the only soluble polymer of this general class of compounds that has been observed to date.

Its enhanced solubility allows for NMR studies in solution both at room and low temperatures. The room temperature ^{31}P NMR spectra of **8** in CD_2Cl_2 or $[D_8]THF/CH_2Cl_2$ (Figure 4, bottom) display a broad signal centered at –196.16 and –235.54 ppm, respectively. Both signals are upfield shifted compared to that reported for the free P_2 ligand **7** (in $[D_6]$acetone/CH_2Cl_2 solution at –157.0 ppm).[15] The broad signals indicate a possible dynamic behavior in solution. Moreover, most likely, **8** is not dissociated into its initial components, as otherwise only a sharp signal of the uncoordinated ligand complex **7** should appear in its room temperature ^{31}P NMR spectrum. When temperatures are lowered to –80 °C or lower in a $[D_8]THF/CH_2Cl_2$ solution, this signal splits into four signals centered at ca. –183, –220, –303 and –320 ppm (Figure 4). These signals are in a similar range as the ones assigned to the atoms P1 and P2 in the ^{31}P MAS-NMR of the polymer **5**. Additionally, these observations reveal that the polymer **8** does not fully stay in its polymeric form in solution, as otherwise only two signals should be present in its low temperature ^{31}P NMR spectrum. Thus, most likely, at least two species with $Cu_xBr_y\{Cp'_2W_2(CO)_4P_2\}_z$ moieties do exist in solutions of **8**, which can explain the very broad signals as being a result of the overlapping of multiple signals in similar regions. The positive ions ESI-MS spectrum of **8** supports the low temperature ^{31}P NMR observations. Here, in contrast to what is observed for the polymers **4**–**6**, the ESI-MS spectrum of **8** shows no decomposition of the $\{Cp'_2W_2(CO)_4P_2\}$ unit, and the most abundant fragments detected are attributable to the cations $[Cu_2Br\{Cp'_2W_2(CO)_4P_2\}_2]^+$, $[Cu\{Cp'_2W_2(CO)_4P_2\}_2]^+$ and

$[Cu\{Cp'_2W_2(CO)_4P_2\}_2(CH_3CN)]^+$. In addition, some other fragments of low abundance attributed to the formula $Cu_nBr_{n-1}\{Cp'_2W_2(CO)_4P_2\}_x$ ($n = 5$, $x = 3$; $n = 4$, $x = 3,2$; $n = 3$, $x = 2$) are also detected. This increased stability of the $\{Cp'_2W_2(CO)_4P_2\}$ unit in **8** is also reflected by the higher melting point (220–222 °C) of **8** as compared to its unsubstituted bromine analogue **5** (120–122 °C). The room temperature ^1H and $^{13}C\{H\}$ NMR spectra of **8** in CD_2Cl_2 show the expected signals attributable to the H and C nuclei of the Cp′ and CO groups of the coordinated P_2 ligand **7**.

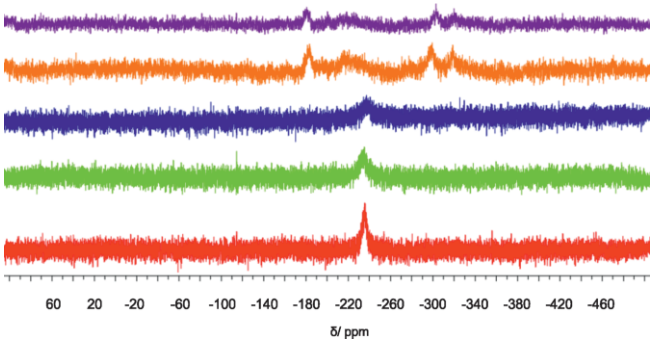

Figure 4. Variable temperature $^{31}P\{^1H\}$ NMR spectrum of polymer **8** in $[D_8]THF/CH_2Cl_2$ (3:1). From bottom to top: 27, 0, –20, –80, –110 °C.

The reaction of **3** with $Ag[CF_3SO_3]$ or $Ag[PF_6]$ in a 1:1 mixture of CH_3CN and CH_2Cl_2 at room temperature allows for the high yield preparation of the dimers **9** (91 %) and **10** (78 %), respectively (Scheme 1, Figure 5). In contrast to the Cu^I polymers **4**–**6**, the Ag^I dimers **9** and **10** are air- and light-stable only for a short time. Solids of **9** and **10** can be indefinitely stored under an inert atmosphere at ambient conditions. As demonstrated for the polymers **4**–**6**, the formation of **9** and **10** also appears to be independent of the reactant stoichiometry. These compounds are obtained regardless of whether a 1:1 or 2:1 reactant stoichiometry is utilized. Compounds **9** and **10** have been characterized by single-crystal X-ray crystallography, and the measurement details are summarized in the ESI. These two compounds are structurally similar to each other and also to the dimers obtained from the reaction of the P_2 ligand complex $[Cp_2Mo_2(CO)_4(\mu,\eta^2{:}\eta^2\text{-}P_2)]$ (**1**) with $Ag[CF_3SO_3]$ or $Ag[PF_6]$, respectively.[11,9a] Both **9** and **10** consist of a dication well separated from the anions (Figure 5). In each compound, the two Ag^I atoms are surrounded by four P_2 ligands **3**, two of which possess a bridging $\mu,\eta^1{:}\eta^1$-coordination mode and the other two of which adopt an η^2-side-on coordination. Hence, each Ag^I ion in **9** and **10** possesses a distorted tetrahedral coordination sphere consisting of four P atoms. The central Ag_2P_4 six-membered rings in **9** and **10** show only a slight distortion towards a chair conformation [folding angles 16.35 (15) and 9.35 (9)°]. The P–P bond lengths in **9** [2.103(3)–2.166(2) Å] and **10** [2.109(2)–2.159(2) Å] are elongated relative to that of the non-coordinated ligand complex **3** [2.095(2) Å] as well as to those in their molybdenum dimer analogues [2.098(2)–2.145(1) Å].[11] The Ag–P bond lengths inside [2.470(2)–2.482(2) Å] and outside [2.603(2)–2.683(1) Å] of the six-membered rings in **9** and **10** are not identical to each other and the Ag···Ag distances (4.630 and 4.558 Å) suggest the absence of argentophilic interaction.[18]

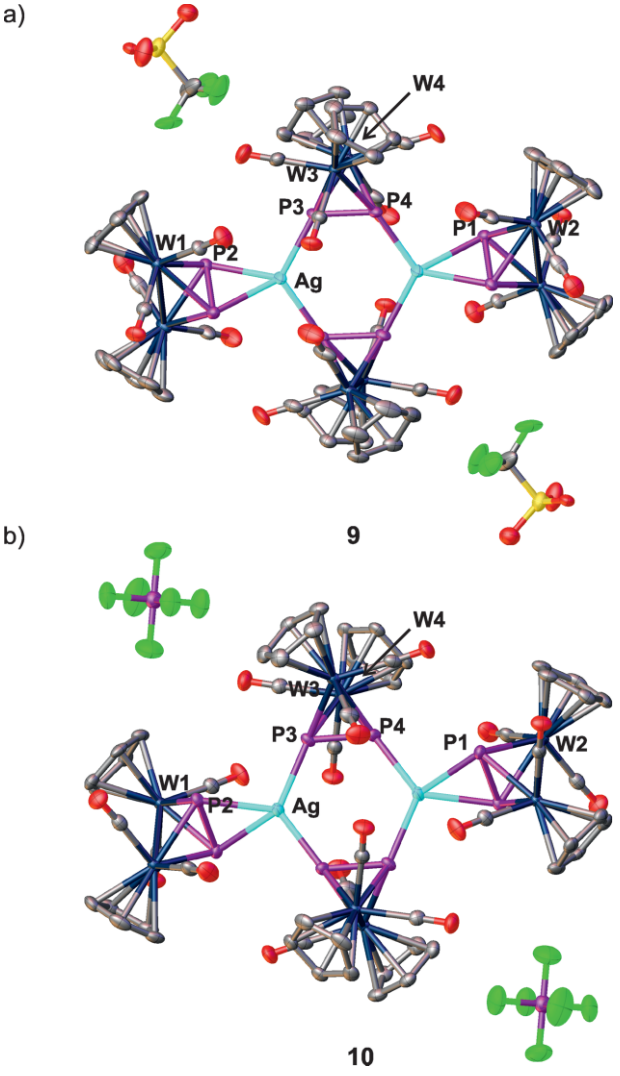

Figure 5. Molecular structure of the dimers a) **9** and b) **10**; H atoms have been omitted for clarity.

Compounds **9** and **10** are only slightly soluble in donor solvents such as CH_3CN but insoluble in other common organic solvents such as CH_2Cl_2, THF, toluene and *n*-pentane. Their room temperature ^{31}P NMR spectra in CD_3CN each show a broad signal centered at δ = –177.2 and –167.8 ppm, respectively, which is upfield shifted compared to that of the free P_2 ligand **3** (in $[D_6]$acetone/CH_2Cl_2: –152.6 ppm).[15] The ESI mass spectra of **9** and **10** in CH_3CN show a main peak in the positive ion mode for the monocation $[Ag\{Cp_2W_2(CO)_4P_2\}_2]$ as well as peaks for smaller fragments indicating a partial dissociation of the dimers **9** and **10** in solutions of CH_3CN. The IR spectra of **9** and **10** exhibit each two strong bands in the range between ca. $\upsilon_{(CO)} \approx 1900$ and 1960 cm^{-1}, which are attributed to the CO moieties of **3**.

Conclusions

The obtained results present the possibility to use the P_2 ligand complex $[Cp_2W_2(CO)_4(\mu,\eta^2{:}\eta^2\text{-}P_2)]$ (**3**) and its better soluble analogue $[Cp'_2W_2(CO)_4(\mu,\eta^2{:}\eta^2\text{-}P_2)]$ (**7**) as connecters in supramolec-

ular chemistry. The reaction of **3** with copper halides leads to the novel insoluble linear 1D polymeric compounds $[Cu(\mu\text{-}X)\{Cp_2W_2(CO)_4(\mu,\eta^2{:}\eta^2{:}\eta^1{:}\eta^1\text{-}P_2)\}]_n$ [X = Cl (**4**), Br (**5**), I (**6**)]. The reaction of **7** with CuBr leads to the unprecedented soluble 1D polymer $[Cu(\mu\text{-}Br)\{Cp'_2W_2(CO)_4(\mu,\eta^2{:}\eta^2{:}\eta^1{:}\eta^1\text{-}P_2)\}]_n$ (**8**). The X-ray structures of the polymers **4**–**6** show similar structural motifs with some differences in the arrangements of the CO ligands, decisively influencing their ^{31}P MAS-NMR spectra. A tremendous downfield shift of the signal of one P atom in the spectra of both **4** and **5** are detected, whereas, in **6**, both P atoms are influenced by the CO ligands in the same manner. Owing to the enhanced solubility characteristics of **8**, NMR studies in solutions both at room and low temperatures were conducted, which support a dynamic behavior of this compound in solution. Compound **3** reacts also with the Ag^I salts $Ag[CF_3SO_3]$ and $Ag[PF_6]$, respectively, to give the metal dimers $[Ag_2(\{Cp_2Mo_2(CO)_4(\mu,\eta^2{:}\eta^2{:}\eta^2\text{-}P_2)\}_2)$ $(\{Cp_2Mo_2(CO)_4(\mu,\eta^2{:}\eta^2{:}\eta^1{:}\eta^1\text{-}P_2)\}_2)][X']_2$ {X′ = $[CF_3SO_3]^-$ (**9**), $[PF_6]^-$ (**10**)}. These new results show the versatility of our approach using P-donating ligand complexes in coordination-driven self-assembly reactions, leading to new and unprecedented supramolecular compounds. Current investigations in this field involve multi-component reactions of the P_2-ligand complex (**3**) with metal salts and multitopic organic ligands to yield a new library of organometallic-organic hybrid polymers.

Experimental Section

General Remarks: All manipulations were carried out under dry nitrogen atmosphere using standard glove-box and Schlenk techniques. All solvents were freshly distilled from appropriate drying agents prior to use. IR spectra were recorded on a Varian FTS-800 spectrometer. ^1H, ^{13}C and ^{31}P NMR spectra were recorded on Bruker Avance 300 or 400 spectrometers. ^1H and ^{13}C NMR chemical shifts were reported in parts per million (ppm) relative to Me_4Si as the external standard. ^{31}P NMR chemical shifts were expressed in ppm relative to external 85 % H_3PO_4 and were decoupled from the protons. For the ESI-MS, a Finnignan Thermoquest TSQ 7000 mass spectrometer was used. Elemental analyses were performed by the microanalytical laboratory of the University of Regensburg.

Reagents: The compounds $[Cp_2W_2(CO)_4(\eta^2\text{-}P_2)]$ (**3**)[15] and **7**[15] were prepared according to literature procedures. $AgSO_3CF_3$ (Fluka), $AgPF_6$ (Aldrich), CuCl (Strem), CuBr (Strem), CuI (Aldrich) were transferred to a glove-box for storage and used as received.

Crystal Structure Analysis: The crystals were selected and mounted on a Gemini Ultra diffractometer equipped with a Ruby CCD detector (**3**, **7**, **8**) or an AtlasS2 CCD detector (**4**, **10**) and a GV50 diffractometer equipped with a TitanS2 CCD detector (**5**, **6**, **9**), respectively. All crystals were kept at T = 123(1) K during data collection. Data collection and reduction were performed with **CrysAlispro** [Version 171.32.15 (**3**), 171.33.41 (**7**, **8**), 171.39.37b (**4**, **10**), 171.40.18c (**5**, **6**, **9**)].[19] For the compounds **3** and **7**, a multi-scan absorption correction was performed using spherical harmonics as implemented in SCALE3 ABSPACK. For the compounds **5**, **6** and **9**, a combination of a numerical absorption correction based on Gaussian integration over a multifaceted crystal model and an empirical absorption correction using spherical harmonics as implemented in SCALE3 ABSPACK was performed. For the compounds **4**, **8** and **10**, an analytical numeric absorption correction using a multifaceted crystal model based on expressions derived by R.C. Clark & J.S. Reid.[Clark, R. C. & Reid, J. S. (1995). Acta Cryst. A51, 887–897] was applied. Using **Olex2**,[20] the structures of **3** and **8** were solved by **SIR97**,[21] of **4** by **ShelXS**[22] and of **5**, **6**, **7**, **9** and **10** by **ShelXT**,[23] respectively. A least-square refinement on F^2 was carried out with **ShelXL**[24] for all structures. All non-hydrogen atoms were refined anisotropically. Hydrogen atoms at the carbon atoms were located in idealized positions and refined isotropically according to the riding model.

CIF files with comprehensive information on the details of the diffraction experiments and full tables of bond lengths and angles for **3**–**8** are deposited in Cambridge Crystallographic Data Centre. CCDC1917256 (for **3**), 1917257 (for **4**), 1917258 (for **5**), 1917259 (for **6**), 1917260 (for **7**), 1917261 (for **8**), 1917262 (for **9**), and 1917263 (for **10**), contain the supplementary crystallographic data for this paper. These data can be obtained free of charge from The Cambridge Crystallographic Data Centre.

Crystal Data of 3: $C_{14}H_{10}O_4P_2W_2$, M_r = 671.86, monoclinic, $C2/_c$ (No. 15), a = 13.4146(3) Å, b = 7.23990(10) Å, c = 16.5646(5) Å, β = 105.621(3)°, $\alpha = \gamma$ = 90°, V = 1549.34(7) Å^3, T = 123(1) K, Z = 4, Z' = 0.5, $\mu(CuK_a)$ = 29.133, 11257 reflections measured, 1349 unique (R_{int} = 0.0370), which were used in all calculations. The final wR_2 was 0.0590 (all data) and R_1 was 0.0225 [$I > 2(I)$].

Crystal Data of 4: $C_{56}H_{40}Cl_4Cu_4O_{16}P_8W_8$, M_r = 3083.40, monoclinic, $P2_1/n$ (No. 14), a = 14.8767(13) Å, b = 7.9598(4) Å, c = 16.0716(10) Å, β = 111.933(9)°, $\alpha = \gamma$ = 90°, V = 1765.4(2) Å^3, T = 123(1) K, Z = 1, Z' = 0.25, $\mu(MoK_a)$ = 14.541, 11646 reflections measured, 5802 unique (R_{int} = 0.0405), which were used in all calculations. The final wR_2 was 0.0940 (all data) and R_1 was 0.0516 [$I > 2(I)$].

Crystal Data of 5: $C_{14}H_{10}BrCuO_4P_2W_2$, M_r = 815.31, monoclinic, $P2_1/n$ (No. 14), a = 14.8265(3) Å, b = 8.00120(10) Å, c = 16.2004(3) Å, β = 111.281(2)°, $\alpha = \gamma$ = 90°, V = 1790.80(6) Å^3, T = 122.97(10) K, Z = 4, Z' = 1, $\mu(CuK_a)$ = 29.062, 10292 reflections measured, 3482 unique (R_{int} = 0.0460), which were used in all calculations. The final wR_2 was 0.0861 (all data) and R_1 was 0.0338 [$I > 2(I)$].

Crystal Data of 6: $C_{16}H_{13}CuINO_4P_2W_2$, M_r = 903.35, triclinic, $P\bar{1}$ (No. 2), a = 7.9940(4) Å, b = 11.4305(4) Å, c = 11.6062(6) Å, α = 84.043(4)°, β = 82.964(4)°, γ = 77.600(4)°, V = 1024.69(8) Å^3, T = 122.97(10) K, Z = 2, Z' = 1, $\mu(CuK_a)$ = 35.009, 8871 reflections measured, 3924 unique (R_{int} = 0.0303), which were used in all calculations. The final wR_2 was 0.0597 (all data) and R_1 was 0.0239 [$I > 2(I)$].

Crystal Data of 7: $C_{44}H_{52}O_8P_4W_4$, M_r = 1568.13, monoclinic, $C2/_c$ (No. 15), a = 30.630(5) Å, b = 7.159(5) Å, c = 24.780(5) Å, α = 90.000(5)°, β = 118.604(5)°, γ = 90.000(5)°, V = 4771(4) Å^3, T = 123(2) K, Z = 4, Z' = 0.5, $\mu(MoK_a)$ = 9.797, 7342 reflections measured, 4088 unique (R_{int} = 0.0259), which were used in all calculations. The final wR_2 was 0.0810 (all data) and R_1 was 0.0282 [$I > 2(I)$].

Crystal Data of 8: $C_{22}H_{26}BrCuO_4P_2W_2$, M_r = 927.52, monoclinic, $C2/_c$ (No. 15), a = 27.4649(8) Å, b = 7.8948(2) Å, c = 24.9063(9) Å, β = 104.649(4)°, $\alpha = \gamma$ = 90°, V = 5224.9(3) Å^3, T = 123(1) K, Z = 8, Z' = 1, $\mu(CuK_a)$ = 20.034, 9051 reflections measured, 4505 unique (R_{int} = 0.0282), which were used in all calculations. The final wR_2 was 0.0798 (all data) and R_1 was 0.0301 [$I > 2(I)$].

Crystal Data of 9: $C_{33.67}H_{27.67}AgCl_{2.66}F_3N_{1.67}O_{11}P_4SW_4$, M_r = 1782.17, triclinic, $P\bar{1}$ (No. 2), a = 12.2663(2) Å, b = 13.3844(2) Å, c = 15.3098(3) Å, α = 112.898(2)°, β = 98.132(2)°, γ = 94.391(2)°, V = 2268.17(7) Å^3, T = 122.95(14) K, Z = 2, Z' = 1, $\mu(CuK_a)$ = 25.453, 27078 reflections measured, 8899 unique (R_{int} = 0.0587), which were used in all calculations. The final wR_2 was 0.1214 (all data) and R_1 was 0.0448 [$I > 2(I)$].

Crystal Data of 10: $Ag_2C_{66.4}Cl_{3.2}F_{12}H_{56.4}N_{4.4}O_{16}P_{10}W_8$, M_r = 3509.64, triclinic, $P\bar{1}$ (No. 2), a = 12.1523(4) Å, b = 13.2691(4) Å, c = 15.2439(5) Å, α = 112.553(3)°, β = 99.491(3)°, γ = 94.543(3)°, V = 2211.47(13) Å^3, T = 123(2) K, Z = 1, Z' = 0.5, μ(MoK_a) = 11.152, 29919 reflections measured, 14578 unique (R_{int} = 0.0320), which were used in all calculations. The final wR_2 was 0.0571 (all data) and R_1 was 0.0313 [$I > 2(I)$].

Solid-State ^{31}P MAS NMR Spectroscopy: Solid-state ^{31}P MAS NMR spectra of the compounds **4**–**6** were recorded at a resonance frequency of 121.49 MHz on a Bruker AVANCE300 solid-state spectrometer equipped with a 2.5-mm NMR probe operating at MAS rotation frequency of 30 kHz. Chemical shifts are referenced to 85 % H_3PO_4 as an external standard.

Synthesis of 4: A solution of CuCl (15 mg, 0.148 mmol) in CH_3CN (7 mL) was layered over a solution of **3** (50 mg, 0.074 mmol) in CH_2Cl_2 (7 mL) at room temperature. The mixture was kept in the dark at room temperature and orange crystals of **4** were formed within four days. The product was filtered, washed with CH_2Cl_2 (10 mL) and then dried under vacuum. Yield: 37 mg (65 %), m.p.: 109 °C (decomp.); ^{31}P MAS NMR (121.5 MHz, room temp.): δ = –194.0 (m), –316.0 (m). Positive ion ESI-MS (CH_3CN + 10 mmol/L $NH_4^+CH_3CO^-$, room temp.): *m/z* (%) 1406.8 (7) $[Cu_2Cl_2\{Cp_4W_4(CO)_3P_2\}]^+$, 775.7 (18) $[CuCl\{Cp_2W_2(CO)_2P_2\}]^+$, 775.5 (100) $[(NH_4)\{Cp_2W_2(CO)_4P_2\}(CH_3CN)_2]^+$, 738.8 (23) $[Cu\{Cp_2W_2(CO)_4P_2\}]^+$, 711.8 (23) $[Cu\{Cp_2W_2(CO)_3P_2\}]^+$.IR (KBr): $\tilde{\nu}$/cm^{-1} = 3110 (w), 2963 (w), 2359 (w), 2340 (w), 2001 (s; CO), 1949 (s; CO), 1921 (s; CO), 1852 (s; CO), 1823 (s; CO), 1416 (m), 1355 (vw), 1261 (m), 1094 (s), 1020 (s), 937 (vw), 866 (w), 847 (m), 799 (s), 703 (w), 606 (w), 575 (w), 545 (w), 511 (m), 474 (s), 438 (m) cm^{-1}. Elemental analysis: calcd. (%) for $C_{28}H_{20}Cl_2Cu_2O_8P_4W_4$ (1541.71): C 21.81, H 1.31; found C 22.05, H 1.52.

Synthesis of 5: A solution of CuBr (21 mg, 0.148 mmol) in CH_3CN (7 mL) was layered over a solution of **3** (50 mg, 0.074 mmol) in CH_2Cl_2 (7 mL) at room temperature. The mixture was kept in the dark at room temperature and red crystals of **4** were formed within four days. The product was filtered and dried under vacuum. Yield: 49 mg (81 %), m.p.: 121 °C (decomp.); ^{31}P MAS NMR (121.5 MHz, room temp.): δ = –195.3 (m), –329.6 (m). Positive ion ESI-MS (CH_3CN + 10 mmol/L $NH_4^+CH_3CO^-$, room temp.): *m/z* (%) 1695.0 (1) $[(NH_4)(CH_3CO)Cu_2Br_2\{Cp_4W_4(CO)_8P_4\}]^+$, 1551.0 (6) $[Cu_2Br_2\{Cp_4W_4(CO)_5P_4\}]^+$, 1407.0 (14) $[CuBr\{Cp_2W_2(CO)P_2\}]^+$, 775.7 (100) $[(NH_4)\{Cp_2W_2(CO)_4P_2\}(CH_3CN)_2]^+$, 747.8 (17) $[(NH_4)\{Cp_2W_2(CO)_6P_2\}]^+$, 719.7 (13) $[(NH_4)\{Cp_2W_2(CO)_5P_2\}]^+$. IR (KBr): $\tilde{\nu}$/cm^{-1} = 3118 (w), 2963 (w), 2002 (s; CO), 1952 (s; CO), 1923 (s; CO), 1850 (s; CO), 1821 (s; CO), 1415 (m), 1261 (s), 1096 (s), 1057 (s), 1022 (s), 845 (m), 802 (s), 707 (vw), 606 (w), 575 (w), 545 (w), 513 (m), 474 (w), 441 (m) cm^{-1}. Elemental analysis: calcd. (%) for $C_{28}H_{20}Br_2Cu_2O_8P_4W_4$ (1630.61): C 20.62, H 1.24; found C 20.65, H 1.61.

Synthesis of 6: A solution of CuI (28 mg, 0.148 mmol) in CH_3CN (7 mL) was layered over a solution of **3** (50 mg, 0.074 mmol) in CH_2Cl_2 (7 mL) at room temperature. The mixture was kept in the dark at room temperature and orange crystals of **6** were formed within two days. The product was filtered and dried under vacuum. Yield: 52 mg (81 %), m.p.: 108 °C (decomp.); ^{31}P MAS NMR (121.5 MHz, room temp.): δ = –209.9 (m). Positive ion ESI-MS (CH_3CN + 10 mmol/L $NH_4^+CH_3CO^-$, room temp.): *m/z* (%) 1596.8 (2) $[Cu_3I_2\{Cp_4W_4(CO)P_4\}]^+$, 1551.0 (1) $[(NH_4)Cu_2I_2\{Cp_4W_4(CO)P_4\}]^+$, 1406.9 (8) $[Cu_2I\{Cp_4W_4(CO)P_4\}]^+$, 967.7 (10) $[Cu_2I(CH_3CN)\{Cp_2W_2(CO)_4P_2\}]^+$, 919.7 (6) $[(NH_4)_2I(CH_3CN)_2\{Cp_2W_2(CO)_4P_2\}]^+$, 775.8 (100) $[NH_4(CH_3CN)_2\{Cp_2W_2(CO)_4P_2\}]^+$, 747.9 (7) $[NH_4(CH_3CN)_2\{Cp_2W_2(CO)_3P_2\}]^+$, 719.9 (6) $[NH_4(CH_3CN)_2\{Cp_2W_2(CO)_2P_2\}]^+$. IR (KBr): $\tilde{\nu}$/cm^{-1} = 3118 (w), 2963 (w), 2361 (w), 2285 (w), 2251 (w), 1986 (s; CO), 1973 (s; CO), 1916 (s; CO), 1867 (s; CO), 1417 (m), 1261 (m), 1105 (m), 1060 (m), 1025 (w), 1012 (m), 916 (w), 863 (w), 850 (m), 829 (s), 804 (m), 560 (m), 526 (m), 496 (m), 471 (m), 454 (m) cm^{-1}. Elemental analysis: calcd. (%) for $C_{28}H_{20}I_2Cu_2O_8P_4W_4(CH_3CN)$ (1765.66): C 21.27, H 1.45, N 1.55; found C 21.33, H 1.70, N 1.43.

Synthesis of 8: A solution of CuBr (20 mg, 0.069 mmol) in CH_3CN (4 mL) was added to a solution of **7** (50 mg, 0.069 mmol) in CH_2Cl_2 (5 mL). The mixture was then stirred for one hour at room temperature and then layered with three-fold of *n*-pentane. Within seven days, orange crystals of **8** were formed, filtered and finally dried under vacuum. Yield: 55 mg (86 %), m.p.: 221 °C (decomp.). ^{1}H NMR (400.1 MHz, CD_2Cl_2, 27 °C): δ = 5.46 (t, $^3J_{(H,H)}$ = 2.50 Hz, 2H, C_5H_5), 5.32 (t, $^3J_{(H,H)}$ = 2.50 Hz, 2H, C_5H_5), 1.34 (s, 9H, *t*Bu) (s) ppm. ^{13}C{^{1}H} NMR (100.63 MHz, CD_2Cl_2, 27 °C): δ = 210.5 (s, CO), 119.1 (s, C_5H_5), 87.9 (s, C_5H_5), 83.2 (s, C_5H_5), 31.9 (s, *t*Bu), 31.8 (s, *t*Bu) ppm. ^{31}P NMR (161.95 MHz, CD_2Cl_2, 27 °C): δ = –196.16 (s) ppm. ^{31}P NMR (161.95 MHz, [D$_8$]THF/CH_2Cl_2 (3:1), 27 °C): δ = –235.54 (s) ppm. ^{31}P NMR (161.95 MHz, [D$_8$]THF/CH_2Cl_2 (3:1), 0 °C): δ = –236.34 (s) ppm. ^{31}P NMR (161.95 MHz, [D$_8$]THF/CH_2Cl_2 (3:1), –20 °C): δ = –237.39 (s) ppm. ^{31}P NMR (161.95 MHz, [D$_8$]THF/CH_2Cl_2 (3:1), –80 °C): δ = –183.59 (s), –220.61 (s), –299.64 (s), –318.88 (s) ppm. ^{31}P NMR (161.95 MHz, [D$_8$]THF/CH_2Cl_2 (3:1), –110 °C): δ = –180.95 (s), –218.14 (s), –303.00 (s), –319.90 (s) ppm. Positive ion ESI-MS (CH_2Cl_2/CH_3CN, room temp.): *m/z* (%) 2988.2 (1) $[Cu_5Br_4\{Cp'_2W_2(CO)_4P_2\}_3]^+$, 2844.4 (1) $[Cu_4Br_3\{Cp'_2W_2(CO)_4P_2\}_3]^+$, 2701.7 (1) $[Cu_3Br_2\{Cp'_2W_2(CO)_4P_2\}_3]^+$, 2558.6 (1) $[Cu_2Br\{Cp'_2W_2(CO)_4P_2\}_3]^+$, 2062.6 (2) $[Cu_4Br_3\{Cp'_2W_2(CO)_4P_2\}_2]^+$, 1918.8 (4) $[Cu_3Br_2\{Cp'_2W_2(CO)_4P_2\}_2]^+$, 1775.0 (16) $[Cu_2Br\{Cp'_2W_2(CO)_4P_2\}_2]^+$, 1631.3 (48) $[Cu\{Cp'_2W_2(CO)_4P_2\}_2]^+$, 887.8 (100) $[Cu\{Cp'_2W_2(CO)_4P_2\}CH_3CN]^+$. IR (KBr): $\tilde{\nu}$/cm^{-1} = 2962 (w), 2906 (w), 2364 (w), 2345 (w), 1999 (s; CO), 1943 (s; CO), 1919 (s; CO), 1859 (s; CO), 1479 (w), 1465 (w), 1448 (w), 1399 (w), 1364 (w), 1262 (m), 1148 (w), 1095 (m), 1022 (m), 898 (w), 844 (m), 801 (m), 735 (w), 702 (w), 569 (w), 538 (w), 516 (w), 478 (w), 442 (m) cm^{-1}. Elemental analysis: calcd. (%) for $C_{22}H_{26}BrCuO_4P_2W_2$ (927.52): C 28.49, H 2.83; found C 28.09, H 2.73.

Synthesis of 9: A solution of $Ag[CF_3SO_3]$ (10 mg, 0.037 mmol) in CH_3CN (5 mL) was layered over a solution of **3** (50 mg, 0.074 mmol) in CH_2Cl_2 (7 mL) at room temperature. The flask was left in the dark for one week during which clear orange crystals of **9** were obtained. These crystals were filtered and dried under vacuum. Yield: 53 mg (91 %), m.p.: 120 °C (decomp.); ^{1}H NMR (400.1 MHz, CD_3CN, 27 °C): δ = 5.42 (s, C_5H_5) ppm. ^{13}C{^{1}H} NMR (100.63 MHz, CD_3CN, 27 °C): δ = 85.8 (s, C_5H_5) ppm. ^{31}P NMR (161.95 MHz, CD_3CN, 27 °C): δ = –177.23 (s) ppm. ^{31}F NMR (282.38 MHz, CD_3CN, 27 °C): δ = –78.08 (s, CF_3SO_3) ppm. Positive ion ESI-MS (CH_3CN, room temp.): *m/z* (%) 1451.1 (90) $[\{Cp_2W_2(CO)_4P_2\}_2Ag]^+$, 820.0 (100) $[Cp_2W_2(CO)_4P_2AgCH_3CN]^+$. IR (KBr): $\tilde{\nu}$/cm^{-1} = 3114 (w), 1940 (s; CO), 1901 (s; CO), 1627 (m), 1418 (m), 1356 (w), 1254 (m), 1167 (m), 1106 (w), 1032 (s), 920 (w), 824 (m), 765 (w), 638 (m), 565 (m), 532 (m), 519 (m), 476 (m), 460 (m), 450 (m) cm^{-1}. Elemental analysis: calcd. (%) for $C_{29}H_{20}SF_3AgO_{11}P_4W_4$ (1600.65): C 21.76, H 1.26, S 2.00; found C 21.58, H 1.61, S 1.87.

Synthesis of 10: A solution of $Ag[PF_6]$ (10 mg, 0.037 mmol) in CH_3CN (5 mL) was layered over a solution of **3** (50 mg, 0.074 mmol) in CH_2Cl_2 (7 mL) at room temperature. The flask was left in the dark for one week during which clear orange crystals of **10** were obtained. These crystals were filtered and dried under vacuum. Yield (relative to **3**): 47 mg (78 %), m.p.: 226–232 °C (decomp.); ^{1}H NMR (400.1 MHz, CD_3CN, 27 °C): δ = 5.39 (s, C_5H_5) ppm. ^{31}P NMR (161.95 MHz, CD_3CN, 27 °C): δ = –143.19 (sep, PF_6), –167.81 (s) ppm. Positive ion ESI-MS (CH_3CN, room temp.): *m/z* (%) 1451.1 (100) $[\{Cp_2W_2(CO)_4P_2\}_2Ag]^+$, 819.7 (11) $[Ag(CH_3CN)\{Cp_2W(CO)_2P_2\}]^+$. IR

(KBr): $\tilde{\nu}/cm^{-1}$ = 3121 (w), 2963 (w), 2923 (w), 2853 (w), 2853 (w), 2361 (w), 2342 (w), 1963 (s; CO), 1929 (s; CO), 1420 (w), 1262 (w), 1105 (w), 1064 (w), 1013 (w), 845 (m), 830 (m), 558 (w), 522 (w), 468 (w), 441 (w) cm^{-1}. Elemental analysis: calcd. (%) for $C_{28}H_{20}F_6AgO_8P_5W_4$ (1596.54): C 21.06, H 1.72; found C 21.07, H 1.40.

Acknowledgments

This work was comprehensively supported by the European Research Council through grant ERC-2013-AdG339072. The authors gratefully acknowledge Dr. Christian Gröger for recording the ^{31}P MAS-NMR spectra of compounds **4-6**.

Keywords: Tungsten · Phosphorus · Copper · Silver · NMR spectroscopy

[1] Selected reviews: a) L.-J. Chen, H.-B. Yang, *Acc. Chem. Res.* **2018**, *51*, 2699–2710; b) C. Lescop, *Acc. Chem. Res.* **2017**, *50*, 885–894; c) M. L. Saha, X. Yan, P. Stang, *Acc. Chem. Res.* **2016**, *49*, 2527–2539; d) T. R. Cook, P. Stang, *Chem. Rev.* **2015**, *115*, 7001–7045; e) C. Rest, R. Kandanelli, G. Fernandez, *Chem. Soc. Rev.* **2015**, *44*, 2543–2572; f) L. Xu, Y.-X. Wang, L.-J. Chen, H.-B. Yang, *Chem. Soc. Rev.* **2015**, *44*, 2148–2167; g) M. Han, D. M. Engelhard, G. H. Clever, *Chem. Soc. Rev.* **2014**, *43*, 1848–1860; h) K. Harris, D. Fujita, M. Fujita, *Chem. Commun.* **2013**, *49*, 6703–6712; i) M. M. J. Smulders, I. A. Riddell, C. Browne, J. R. Nitschke, *Chem. Soc. Rev.* **2013**, *42*, 1728–1754.

[2] Selected reviews: a) S. Pullen, G. H. Clever, *Acc. Chem. Res.* **2018**, *51*, 3052–3064; b) T. R. Cook, Y.-R. Zheng, P. J. Stang, *Chem. Rev.* **2013**, *113*, 734–777; c) S. Park, S. Y. Lee, K.-M. Park, S. S. Lee, *Acc. Chem. Res.* **2012**, *45*, 391–403; d) M.-X. Li, H. Wang, S.-W. Liang, M. Shao, X. He, Z.-X. Wang, S.-R. Zhu, *Cryst. Growth Des.* **2009**, *9*, 4626–4633.

[3] a) P. J. Stang, B. Olenyuk, J. Fun, A. M. Arif, *Organometallics* **1996**, *15*, 904–908; b) K. Škoch, I. Císařová, J. Schulz, U. Siemeling, P. Štěpnička, *Dalton Trans.* **2017**, *46*, 10339–10354.

[4] M. Scheer, *Dalton Trans.* **2008**, 4372–4386.

[5] Recent papers: a) M. E. Moussa, M. Fleischmann, E. V. Peresypkina, L. Dütsch, M. Seidl, G. Balázs, M. Scheer, *Eur. J. Inorg. Chem.* **2017**, 3222–3226; b) C. Heindl, A. Kuntz, E. V. Peresypkina, A. V. Virovets, M. Zabel, D. Lüdeker, G. Brunklaus, M. Scheer, *Dalton Trans.* **2015**, *44*, 6502–6509; c) C. Heindl, E. V. Peresypkina, A. V. Virovets, V. Y. Komarov, M. Scheer, *Dalton Trans.* **2015**, *44*, 10245–10252; d) M. Fleishmann, S. Welsch, E. V. Peresypkina, A. V. Virovets, M. Scheer, *Chem. Eur. J.* **2015**, *21*, 14332–14336; e) F. Dielmann, C. Heindl, F. Hastreiter, E. V. Peresypkina, A. V. Virovets, R. M. Gschwind, M. Scheer, *Angew. Chem. Int. Ed.* **2014**, *53*, 13605–13608; *Angew. Chem.* **2014**, *126*, 13823; f) E.-M. Rummel, M. Eckhardt, M. Bodensteiner, E. V. Peresypkina, W. Kremer, C. Gröger, M. Scheer, *Eur. J. Inorg. Chem.* **2014**, 1625–1637; g) H. Krauss, G. Balázs, M. Bodensteiner, M. Scheer, *Chem. Sci.* **2010**, *1*, 337–342.

[6] a) C. Heindl, E. Peresypkina, A. V. Virovets, I. S. Bushmarinov, M. G. Medvedev, B. Krämer, B. Dittrich, M. Scheer, *Angew. Chem. Int. Ed.* **2017**, *56*, 13237–13243; *Angew. Chem.* **2017**, *129*, 13420; b) E. Peresypkina, C. Heindl, A. Virovets, M. Scheer in *Inorganic Superspheres* (Ed.: S. Dehnen), Springer International Publishing, Cham, **2017**, pp. 321–373; c) C. Heindl, E. V. Peresypkina, D. Lüdeker, G. Brunklaus, A. V. Virovets, M. Scheer, *Chem. Eur. J.* **2016**, *22*, 2599–2604; d) C. Heindl, E. V. Peresypkina, A. V. Virovets, W. Kremer, M. Scheer, *J. Am. Chem. Soc.* **2015**, *137*, 10938–10941; e) M. Fleischmann, S. Welsch, H. Krauss, M. Schmidt, M. Bodensteiner, E. V. Peresypkina, M. Sierka, C. Gröger, M. Scheer, *Chem. Eur. J.* **2014**, *20*, 3759–3768; f) M. Scheer, A. Schindler, R. Merkle, B. P. Johnson, M. Linseis, R. Winter, C. E. Anson, A. V. Virovets, *J. Am. Chem. Soc.* **2007**, *129*, 13386–13387; g) J. Bai, A. V. Virovets, M. Scheer, *Science* **2003**, *300*, 781–783.

[7] S. Welsch, C. Gröger, M. Sierka, M. Scheer, *Angew. Chem. Int. Ed.* **2011**, *50*, 1435; *Angew. Chem.* **2011**, *123*, 1471.

[8] a) O. J. Scherer, H. Sitzmann, G. Wolmershäuser, *J. Organomet. Chem.* **1984**, *268*, C9–C12; b) O. J. Scherer, J. Schwalb, H. Sitzmann, *Inorg. Synth.* **1990**, *27*, 224–227; c) L. Y. Goh, C. K. Chu, R. C. S. Wong, T. W. Hambley, *J. Chem. Soc., Dalton Trans.* **1989**, 1951–1956; d) L. Y. Goh, R. C. S. Wong, *Inorg. Synth.* **1992**, *29*, 247–250.

[9] a) J. Bai, E. Leiner, M. Scheer, *Angew. Chem. Int. Ed.* **2002**, *41*, 783–786; *Angew. Chem.* **2002**, *114*, 820; b) M. Scheer, L. Gregoriades, J. Bai, M. Sierka, G. Brunklaus, H. Eckert, *Chem. Eur. J.* **2005**, *11*, 2163–2169; c) M. Scheer, L. J. Gregoriades, M. Zabel, M. Sierka, L. Zhang, H. Eckert, *Eur. J. Inorg. Chem.* **2007**, 2775–2782.

[10] I. Krossing, *Chem. Eur. J.* **2001**, *7*, 490–502.

[11] M. Scheer, L. J. Gregoriades, M. Zabel, J. Bai, I. Krossing, G. Brunklaus, H. Eckert, *Chem. Eur. J.* **2008**, *14*, 282–295.

[12] M. Elsayed Moussa, S. Welsch, L. J. Gregoriades, G. Balázs, M. Seidl, M. Scheer, *Eur. J. Inorg. Chem.* **2018**, 1683–1687.

[13] a) P. Sekar, M. Scheer, A. Voigt, R. Kirmse, *Organometallics* **1999**, *18*, 2833–2837; b) P. Sekar, S. Umbarkar, M. Scheer, A. Voigt, R. Kirmse, *Eur. J. Inorg. Chem.* **2000**, 2585–2589.

[14] a) M. Elsayed Moussa, E. Peresypkina, A. V. Virovets, D. Venus, G. Balázs, M. Scheer, *CrystEngComm* **2018**, *20*, 7417–7422; b) M. Elsayed Moussa, M. Seidl, G. Balázs, M. Zabel, A. V. Virovets, B. Attenberger, A. Schreiner, M. Scheer, *Chem. Eur. J.* **2017**, *23*, 16199–16203; c) M. Elsayed Moussa, B. Attenberger, E. M. Fleischmann, A. Schreiner, M. Scheer, *Eur. J. Inorg. Chem.* **2016**, 4538–4541; d) M. Elsayed Moussa, B. Attenberger, E. V. Peresypkina, M. Fleischmann, G. Balázs, M. Scheer, *Chem. Commun.* **2016**, *52*, 10004–10007; e) B. Attenberger, E. V. Peresypkina, M. Scheer, *Inorg. Chem.* **2015**, *54*, 7021–7029; f) B. Attenberger, S. Welsch, M. Zabel, E. Peresypkina, M. Scheer, *Angew. Chem. Int. Ed.* **2011**, *50*, 11516–11519; *Angew. Chem.* **2011**, *123*, 11718.

[15] J. Schwalb, *Chrom- und Wolframkomplexe mit P_x-Liganden*. Universität Kaiserslautern, Kaiserslautern, **1988**.

[16] J. E. Davies, M. J. Mays, P. R. Raithby, G. P. Shields, P. K. Tompkin, A. D. Woods, *J. Chem. Soc., Dalton Trans.* **2000**, 1925–1930.

[17] J. E. Davies, M. C. Klunduk, M. J. Mays, P. R. Raithby, G. P. Shields, P. K. Tompkin, *J. Chem. Soc., Dalton Trans.* **1997**, 715–720.

[18] H. Schmidbaur, A. Schier, *Angew. Chem. Int. Ed.* **2015**, *54*, 746–784; *Angew. Chem.* **2015**, *127*, 756.

[19] *CrysAlisPro* Software System, Rigaku Oxford Diffraction, (**2008**–2018).

[20] O. V. Dolomanov, L. J. Bourhis, R. J. Gildea, J. A. K. Howard, H. Puschmann, *J. Appl. Crystallogr.* **2009**, *42*, 339–341.

[21] A. Altomare, M. C. Burla, M. Camalli, G. L. Cascarano, C. Giacovazzo, A. Guagliardi, A. G. G. Moliterni, G. Polidori, R. Spagna, *J. Appl. Crystallogr.* **1999**, *32*, 115–119.

[22] G. M. Sheldrick, *Acta Crystallogr., Sect. A* **2008**, *64*, 112–122.

[23] G. M. Sheldrick, *Acta Crystallogr., Sect. A* **2015**, *71*, 3–8.

[24] G. M. Sheldrick, *Acta Crystallogr., Sect. C* **2015**, *71*, 3–8.

Received: May 23, 2019